

# Photodegradation of Thermodegraded Polypropylene/High-Impact Polystyrene Blends: Mechanical Properties

L. L. Fernandes, C. A. Freitas, N. R. Demarquette, G. J. M. Fechine\*

*Metallurgical and Materials Engineering Department, University of São Paulo, Avenida Professor Melo Moraes 2463, São Paulo 05508-900, Brazil*

Received 5 November 2009; accepted 9 July 2010

DOI 10.1002/app.33096

Published online 3 November 2010 in Wiley Online Library (wileyonlinelibrary.com).

**ABSTRACT:** The influence of the addition of high-impact polystyrene (HIPS) on polypropylene (PP) photodegradation was studied with blends obtained by extrusion with and without styrene-butadiene-styrene (SBS) copolymer (10 wt % with respect to the dispersed phase). The concentrations of HIPS ranged from 10 to 30 wt %. The blends and pure materials were exposed for periods of up to 15 weeks of UV irradiation; their mechanical properties (tensile and impact), fracture surface, and melt flow indices were monitored. After 3 weeks of UV exposure, all of the materials presented mechanical properties of the same order of magnitude. However, for times of exposure greater than 3 weeks, an

increasing concentration of HIPS resulted in a better photostability of PP. These results were explained in light of morphological observations. This increase of photostability was even greater when SBS was added to the blends. It was more difficult to measure the melt flow index of the binary PP/HIPS blends than that of PP for low concentrations of HIPS; this was most likely due to energy transfer between the blend domains during photodegradation. This phenomenon was not observed for the ternary blends. © 2010 Wiley Periodicals, Inc. *J Appl Polym Sci* 120: 770–779, 2011

**Key words:** blends; degradation; polyolefins

## INTRODUCTION

Plastic materials represent the largest volume of solid waste because of their relative low density. Moreover, they can stay nondegraded for more than 50 years, and solutions to decrease the volume of their waste, such as recycling and the use of biodegradable polymers, have been suggested for the last decade.<sup>1–4</sup> Mechanical recycling is one of the most used alternatives for transforming plastic wastes into new products and is mainly used in the case of polyolefins and poly(ethylene terephthalate). Polypropylene (PP), a semicrystalline polymer with a wide range of applications, such as in the packaging and automotive industries, is one of the most widely used commodity plastics. As an example, its annual U.S. consumption for bottles in 2004 was 190,000,000 pounds, and the amount recycled was 6,000,000 pounds.<sup>5</sup> PP is easily recyclable and may be reprocessed for use in less noble applications. However,

this mechanical recycling results in a decrease in the mechanical properties because of a decrease in the molar mass during thermomechanical treatment. Also, the resulting material may suffer photooxidation during its shelf life; this drastically reduces its properties. To cope with these problems, it is possible to blend PP with another polymer to increase its mechanical properties and maybe its resistance to UV radiation. In particular, it is possible to blend it with high-impact polystyrene (HIPS).<sup>6,7</sup>

The photodegradation of homopolymers, such as PP<sup>8–10</sup> and HIPS,<sup>11–14</sup> is very well known; however, very little is known about the photodegradation of the blends. During the photodegradation process of PP, chain scissions, the generation of carbonyl groups and surface cracks, and a decrease in the mechanical properties are generally observed.<sup>1–3</sup> In the case of HIPS, chain scissions and crosslinking reactions generally occur within the polystyrene and polybutadiene phases, respectively.<sup>11–14</sup> In the case of the photodegradation of the blends, very few studies have been conducted.<sup>15–20</sup> In some cases, it has been shown that the photodegradation of blends follows one of the two polymers of the blends,<sup>15</sup> but in most studies, it has been shown that the extent of the photodegradation of a blend depends on its morphology. This was proven to be true for poly(vinyl chloride)/poly(ethylene oxide), poly(vinyl chloride)/poly(vinyl alcohol), poly(methyl methacrylate)/polystyrene (PS), and poly(vinyl acetate)/PS.<sup>16–18</sup> In turn, the blend morphology can be controlled during its processing by the rheological properties of the

\*Present address: Department of Materials Engineering, Mackenzie Presbyterian University, Rua da Consolação 930, São Paulo, Brazil 01302-907.

Correspondence to: N. R. Demarquette (nick@usp.br) or G. J. M. Fechine (guilherminojm@mackenzie.br).

Contract grant sponsors: Fundação de Amparo à Pesquisa do Estado de São Paulo, Coordenação de Aperfeiçoamento de Pessoal de Nível Superior, Conselho Nacional de Desenvolvimento Científico e Tecnológico.

components, blend composition, and addition of a compatibilizer. The addition of this compatibilizer normally results in a finer and more homogeneous morphology, a better adhesion between the polymers forming the blend, and better engineering properties.<sup>21,22</sup>

More recently, it has been shown that photodegradation in blends occurs under the effects of interactions, such as an exchange of energy in excited state between the polymers forming the blends.<sup>19,20</sup> This effect of interaction can be altered by the presence of a compatibilizer within the blend.<sup>20</sup>

However, almost no studies have reported the effect of photodegradation on the mechanical properties. To our knowledge, the only authors who presented the effect of photodegradation on the mechanical properties of these blends were Saron et al.,<sup>19</sup> who studied the effect of photodegradation on blends of poly(2,6-dimethyl-1,4 phenylene oxide) (HIPS).<sup>19</sup>

In this study, a commercial sample of PP was purposely thermomechanically (PP<sub>thermo</sub>) degraded (to simulate mechanical recycling) and mixed with HIPS; this resulted in blends with concentrations ranging from 90/10 to 70/30 (matrix of PP). Styrene-butadiene-styrene (SBS) copolymer was added to the blend to act as a compatibilizer to improve the adhesion between the phases and the mechanical properties. The pure materials and noncompatibilized and compatibilized blends were then exposed to UV light for various irradiation intervals, and their mechanical properties were monitored as a function of time and examined in light of the melt flow index (MFI) and morphology of surface fracture.

## EXPERIMENTAL

### Materials

In this study, commercial PP with an MFI of 1.3 g/10 min and HIPS with an MFI of 12 g/min were used. SBS copolymer was used as a compatibilizer for the blend. According to the manufacturer, the polymers did not contain UV stabilizers. PP was purposely thermally degraded by processing five times in a Rheomix PTW 16 twin-screw extruder (Karlsruhe, Germany) of a Haake PolyLab 900 torque rheometer (Karlsruhe, Germany). The screw temperatures were set to 190, 200, 220, and 220°C, and the speed was set to 100 rpm. These procedures led to an increase in the MFI of PP to 3.8 g/10 min. The blends were prepared with the same screw extruder, but the extruder temperatures and screw speed were modified to 180, 200, 200, and 200°C and 70 rpm, respectively. Three binary PP/HIPS blends containing 30, 20 and 10 wt % of HIPS (70/30, 80/20 and 90/10, respectively) were prepared. Three ternary blends (with the same PP/HIPS compositions), to

which SBS was added, were also prepared. The SBS was first mixed with the dispersed phase at a concentration of 10 wt % with respect to the dispersed phase and extruded. For all binary blends, the dispersed phase, HIPS, was also extruded before it was blended with PP for the sake of comparison. Injection-molded samples were then obtained with a DEMAG injection-molding machine (Wiehe, Germany) with dimensions according to ASTM D 638 and D 256 for the tensile and impacts tests, respectively. The profile of temperatures was 180, 180, 185, and 190°C, and the mold temperature was 45°C.

### Photooxidation conditions

The injection-molded samples (tensile and impact) were exposed to UV light in a Q-Lab weathering chamber with Q-Panel UVA fluorescent lamps (Cleveland, Ohio, USA). These lamps were 1.2 m long and produced UV light that matched reasonably well with sunlight with a cutoff at 290 nm. The weathering cycle was defined as follows: 8 h under UV light at 60°C and 4 h in the dark under condensed water at 50°C. The irradiation intensity reaching the sample surface was 0.89 W/m<sup>2</sup>. Under these conditions, the specimens were submitted to a combination of photodegradation, thermal degradation, and hydrolytic degradation; we offered very harsh conditions for sample deterioration. In the results shown later, the exposure time is reported as the number of weeks.

### Characterization

We analyzed the morphology of the blends by observing the cryogenic fractures of the impact samples by scanning electron microscopy (SEM) with a Phillips XL30 scanning electron microscope (Eindhoven, Netherlands) operating at 15 kV. The samples were covered with gold with a Balzers sputter coater (model SCD-050, Liechtenstein, Switzerland). Quantitative analysis of the morphology was performed with Carl Zeiss Vision KS-300 software (Nagano, Japan), and Saltikov's correction was used.

Before and after various exposure times, the samples were analyzed by different methods of characterization. For tensile strength measurements, the samples were tested in a Kratos K 2.000MP machine (Cotia, São Paulo, Brazil) operating at crosshead speeds of 1 and 20 mm/min at 25°C. The speed of 1 mm/min was used to calculate Young's modulus. For Izod impact strength tests, unnotched samples were tested in a Tinius Olsen IT 504 machine (Charlotte, North Carolina, USA) at 25°C. The choice for unnotched impact test samples relied on the fact that the notched surfaces underwent nonhomogeneous UV degradation as the degradation was more severe at the notch location. The values of tensile

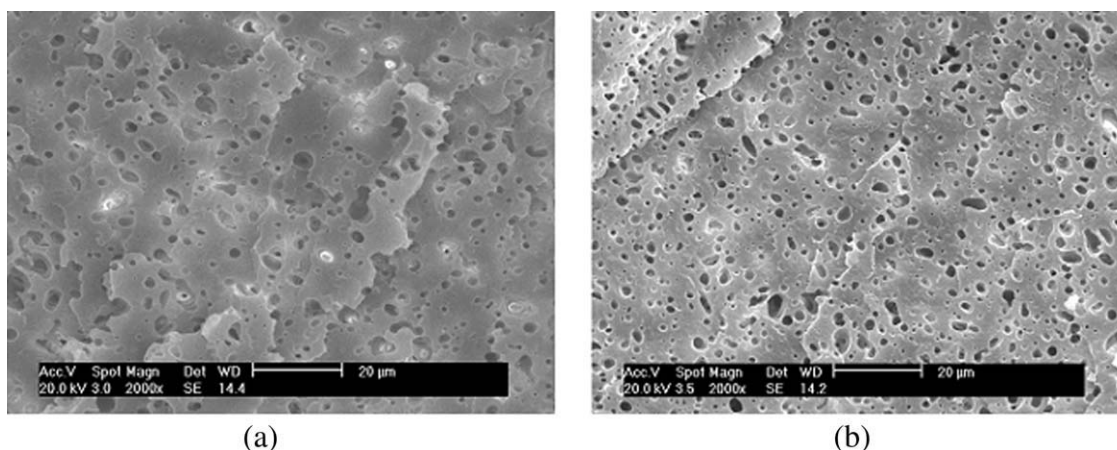


**Figure 1** Morphology of the 70/30 blend (a) without and (b) with the addition of SBS.

strength, elongation, and impact strength reported here represent the averages of at least five samples. The impact strength of the specimen surfaces after testing were analyzed by SEM according to the procedures reported previously. To understand the changes undergone by the polymers during photodegradation, the MFIs of all of the materials (PP, HIPS, and blends) were evaluated with a Ceast melt flow indexer (Modular line, Pianezza, Italy) to get insight on chain scission and, therefore, on molar mass. For the sake of comparison, it was necessary to adopt a single-test condition. The MFIs of the different materials were measured at a temperature of 200°C and with a weight of 5 kg. This condition corresponded to the one used to measure MFI of HIPS and did not correspond to the one that should be used for PP according to the norms. Also, we monitored the chemical changes by Fourier transform infrared (FTIR) spectroscopy by recording the carbonyl index as a function of exposure time. The spectra were obtained from KBr discs with a Nicolet Magna IR-560 (Madison, WI, USA) with a resolution of 2 cm<sup>-1</sup>.

## RESULTS AND DISCUSSION

### Mechanical properties and morphology of PP, HIPS, and their blends before UV exposure

Figure 1(a,b) shows the typical morphologies of the blends obtained in this study. Figure 1(a) shows the morphology of a 70/30 blend without the addition of SBS, and Figure 1(b) shows the morphology of the same composition blend with SBS was added. The micrographs were taken after the dissolution of the HIPS phase in tetrahydrofuran for 3 days. A droplet dispersion morphology was observed in both micrographs. Figure 1(b) indicates that the size of the dispersed phase was slightly reduced upon the addition of SBS. A quantitative analysis showed

that the average diameter of the dispersed droplets decreased from 11 to 8 μm.

Table I presents the mechanical properties (tensile and impact) for PP, HIPS, and the different blends obtained in this study. The binary blends presented lower mechanical properties than the individual components, most likely because of the lack of adhesion between the phases. As also shown in Table I, the increase in the concentration of HIPS within the blend resulted in a decrease in the impact strength. It is well known that the addition of a rubbery phase results in the improvement of the impact strength of the matrix if the interparticle distance (between the nodules of the dispersed phase) is smaller than a critical value.<sup>23,24</sup>

When the concentration of HIPS was increased, the droplets of the dispersed phase probably coalesced, increasing the interparticle distance and turning the blends less tough. Upon addition of SBS, the modulus of elasticity and tensile strength decreased, and the strain at break and impact strength improved. This could have been due to the better adhesion between the phases that was promoted by the addition of SBS (this normally happens between styrenic polymers and polyolefins<sup>25</sup>) and/or because of the incorporation of another rubbery component in the blend, even at low concentrations.<sup>26</sup>

### Photodegradation of the noncompatibilized blends

Figure 2(a–d) shows the mechanical properties for PP<sub>thermo</sub>, HIPS, and different noncompatibilized blends studied here as a function of time of UV exposure. The data of impact strength before any UV exposure for PP and HIPS are not reported on Figure 2(d) because the samples did not break. For PP<sub>thermo</sub>, the modulus of elasticity decreased drastically, whereas for HIPS, it slightly increased as a function of time of UV exposure. For both PP<sub>thermo</sub> and HIPS, the stress, strain at break, and impact resistance decreased as a function of time of UV

TABLE I  
Mechanical Properties of PP, HIPS, and Their Blends

Material	Elastic modulus (GPa)	Stress at the break point (MPa)	Strain at the break point (%)	Impact strength (J/m)
Homopolymers				
PP <sub>thermo</sub>	1.12 ± 0.04	29.4 ± 0.55	348.0 ± 35.0	Partial break
HIPS	1.30 ± 0.02	30.00 ± 0.06	34.1 ± 3.0	No break
Noncompatibilized blends (PP/HIPS)				
70/30	1.09 ± 0.05	19.90 ± 0.72	15.60 ± 0.54	503 ± 38
80/20	1.14 ± 0.03	17.60 ± 0.32	25.15 ± 2.91	681 ± 20
90/10	1.12 ± 0.03	17.22 ± 1.18	28.85 ± 2.67	957 ± 38
Compatibilized blends (PP/HIPS)				
70/30	1.00 ± 0.01	16.8 ± 0.44	32.36 ± 1.16	Partial break
80/20	0.94 ± 0.04	17.12 ± 0.41	34.00 ± 2.25	No break
90/10	1.08 ± 0.07	17.70 ± 0.24	37.70 ± 1.87	No break

exposure. The decrease in the modulus of elasticity and other mechanical properties for PP<sub>thermo</sub> could be easily understood, as the photooxidation mechanism of PP was governed by chain scissions, which led to a decrease in the mechanical properties.<sup>8,10,27,28</sup> In the case of HIPS, the increase in the

modulus of elasticity could be explained by the crosslinking of the rubber phase during photodegradation,<sup>13</sup> whereas the decreases in stress, strain at break, and impact resistance could be explained by the chain scissions of PS undergone during photodegradation.<sup>14,29</sup>

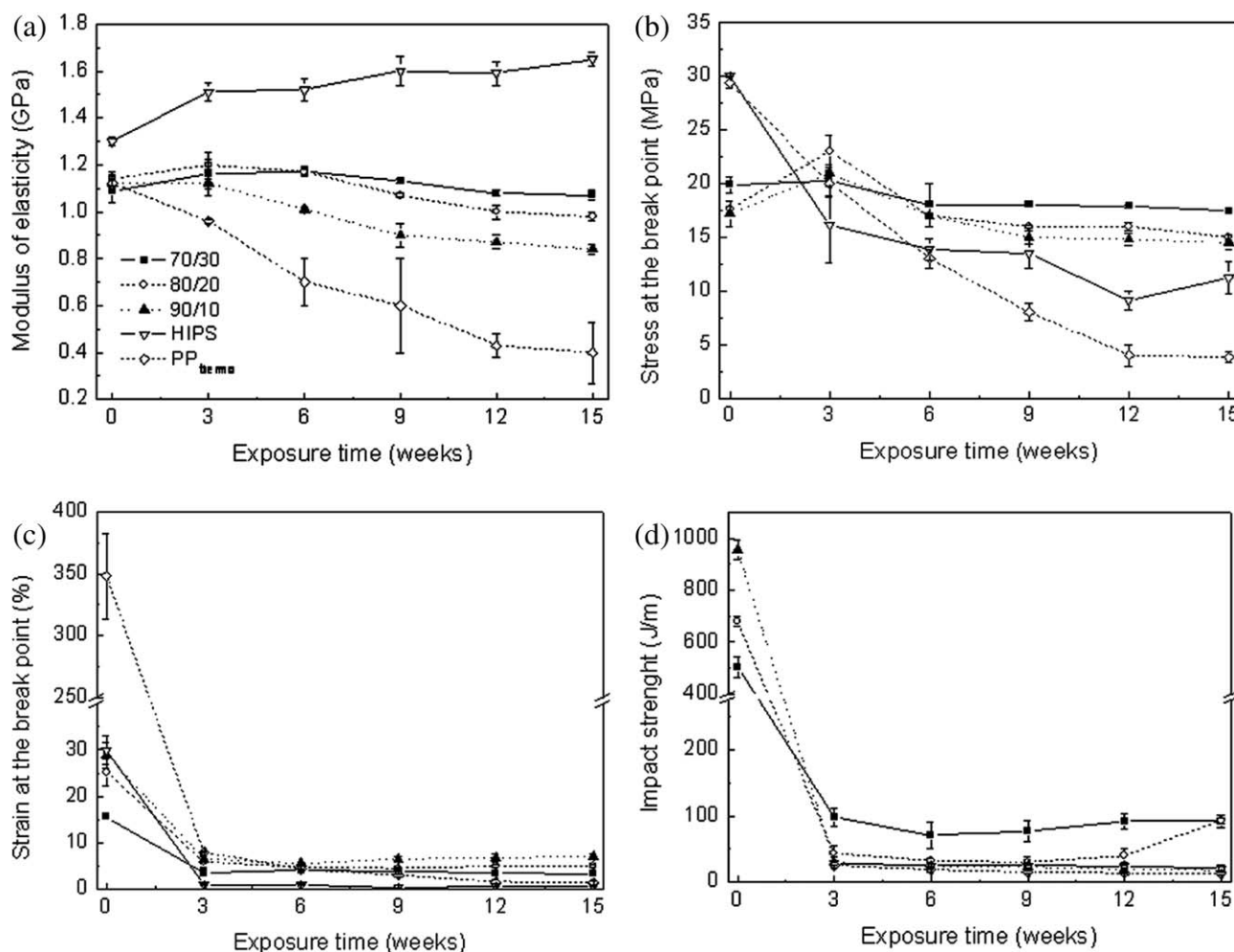
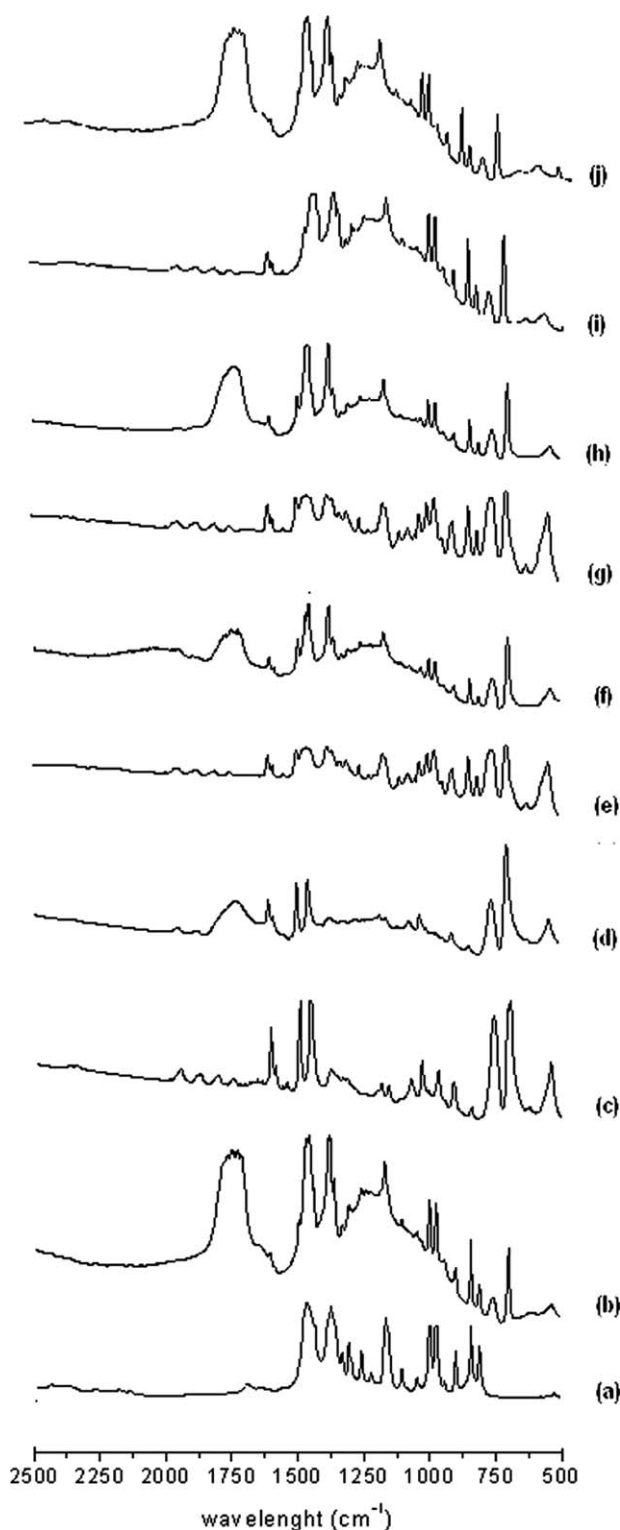


Figure 2 Mechanical properties of PP<sub>thermo</sub>, HIPS, and different noncompatibilized blends: (a) modulus of elasticity, (b) stress at the break point, (c) strain at the break point, and (d) impact strength as functions of the time of UV exposure.





**Figure 3** FTIR spectra of the (a) unexposed PP<sub>thermo</sub>, (b) PP<sub>thermo</sub> exposed for 15 weeks, (c) unexposed HIPS, (d) HIPS exposed for 15 weeks, (e) unexposed 70/30 blend, (f) 70/30 blend exposed for 15 weeks, (g) unexposed 80/20 blend, (h) 80/20 blend exposed for 15 weeks, (i) unexposed 90/10 blend, and (j) 90/10 blend exposed for 15 weeks.

Figure 3 shows the IR spectra of nonexposed and exposed PP, HIPS, and all of the blends. The spectra show a region between 2500 and 500  $\text{cm}^{-1}$  to emphasize the carbonyl group bands (1700–1800  $\text{cm}^{-1}$ ), which were the main chemical group generated during the photodegradation process of PP and HIPS.<sup>8–14</sup> After any duration of photodegradation, all of the samples presented an expressive carbonyl band. A quantitative analysis of these spectra was not attempted, as the spectra were obtained with KBr discs and because it was impossible to identify whether the carbonyl band originated from the degradation of either PP or HIPS. Also, to perform that quantitative analysis, a reference peak needed to be used for normalization. In the case of the two polymers forming the blend studied here, the reference peak differed: the one for PP was 2720  $\text{cm}^{-1}$ ,<sup>10</sup> and the one for HIPS was 1940  $\text{cm}^{-1}$ .<sup>14</sup> This made the quantitative analysis difficult.

The results presented Figure 3, therefore, only indicate that the presence of HIPS did not alter the photooxidation mechanism of PP and vice versa as no other new bands, besides the carbonyl bands, could be identified after photodegradation. However, these results do not show how HIPS influenced the photooxidation process of PP, as a quantitative analysis could not be performed as explained.

Figure 4 shows the MFIs, which could be used as indices to access the change in molar mass of the different materials as a function of time of UV exposure. As shown, for all of materials, the MFI increased as a function of time of UV exposure; however, the increase for PP<sub>thermo</sub> was larger than for HIPS, and it was not possible to measure the MFI of the PP samples that were exposed for times larger than 6 weeks. This could be explained by the thermodegradation that occurred during the MFI

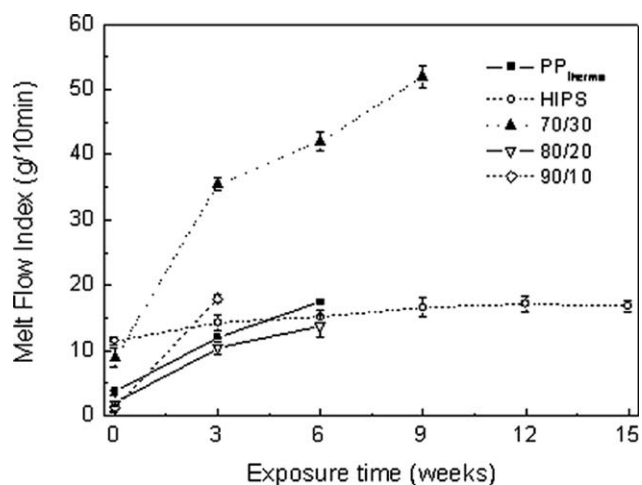


**Figure 4** MFIs for PP<sub>thermo</sub>, HIPS, and different noncompatibilized blends as a function of the time of UV exposure.

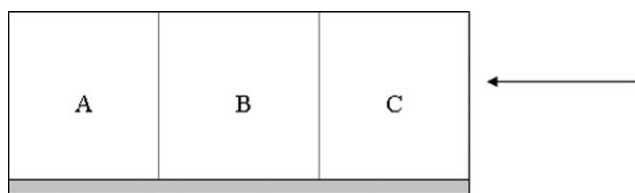


**Figure 5** Illustration of the transversal regions of the impact samples according to SEM analysis.

measurements of those samples. MFI analysis is done at high temperatures and under shear stress. At the beginning of the test, the sample is exposed to high temperatures for some time (typically, 6–7 min) before analysis to reach thermal equilibrium. Carbonyl ( $\sim 1730\text{ cm}^{-1}$ ) and hydroperoxyl groups ( $\sim 3500\text{ cm}^{-1}$ ) were generated during the UV exposure of PP and HIPS, as shown in Figure 3.<sup>10,14</sup> These groups are very sensible to high temperatures,<sup>30</sup> and during MFI analysis, these groups may have caused thermodegradation *in situ* and made the measurement impossible.

As also shown in Figure 4, after UV exposure, the MFI values increased for all of the blends. The measurements were only possible for the blends samples that had undergone 3 (90/10), 6 (80/20), and 9 (70/30) weeks of UV exposure. As mentioned previously, the difficulty in measuring MFI was most likely due to the thermodegradation undergone by the samples during MFI measurements due to the presence of carbonyl and hydroperoxyl groups. The results presented in Figure 4 indicate that it was more difficult to evaluate MFI for the 90/10 and 80/20 blends than for pure PP. These results indicate that the formation of carbonyl and hydroperoxyl groups was larger for the 90/10 and 80/20 blends than for pure PP. These results corroborated the considerations of Waldman and De Paoli,<sup>20</sup> who showed that the increase in carbonyl groups of PP/PS blends was higher than of the one of both homopolymers during the photodegradation process. They explained this phenomenon through the energy transfer between the blend domains and observed that the amount of carbonyls increased with increasing proportion of PP. However, in this study, the difficulty encountered in measuring MFI decreased with increasing dispersed phase concentration. The difference observed between the results presented here and the ones of Waldman and de Paoli<sup>20</sup> could be explained by the difference in the thickness of the samples exposed to UV light. In the case of the samples of PP/PS (containing 15, 30, or 45 wt % PS) tested by de Waldman and Paoli, the thickness of the samples tested was 30  $\mu\text{m}$ , whereas it was 3 mm in this study. In the case of the samples used in this study, UV degradation did not reach the bulk of the sample, as the samples exposed in

this study got more and more opaque as the concentration of HIPS increased.

As shown in Figure 2, the moduli of the blends were intermediate to the ones of PP<sub>thermo</sub> and HIPS, and the other mechanical properties of the blends decreased less with time of UV exposure than the ones of PP<sub>thermo</sub> and HIPS. In particular, after 15 weeks of exposure, the blends showed greater mechanical properties than both PP<sub>thermo</sub> and HIPS (with the exception of the impact strength for the 90/10 blend). This could have been due to the better photostability of the blends compared to that of the individual components or to the opacity of the blends. Because of the opacity of the blends samples, UV radiation may not have penetrated as easily in the homopolymers (the samples were 3 mm thick), which reduced its effect. As HIPS was added to the blend, there was a larger scattering effect of the interface between the polymers forming the blend; this prevented the penetration of the UV radiation within the sample and, therefore, generated a gradient of degradation within the sample.

Figure 5 presents a schematic representation of the regions of impact specimen fracture surfaces analyzed by SEM. The fracture surfaces observed represent cross sections of the specimens. Region A of the fracture surface represents the region opposite to the one hit by the striker. Region B is the crack-propagation zone, and region C represents the crack-initiation zone. The bottom of the fracture surface (the gray line in Fig. 5) represents the region of direct exposure to UV radiation.

Figure 6 shows the micrographs of PP<sub>thermo</sub>, HIPS, and the blends exposed to UV radiation for 3 and 15 weeks from the crack-initiation zone. The nonexposed samples of PP<sub>thermo</sub> and HIPS are not presented here. They did not fracture during the impact tests because the unnotched PP<sub>thermo</sub> and HIPS samples presented high ductility and impact strengths. Figure 6(a,c,e,g,i) shows samples exposed for 3 weeks, and Figure 6(b,d,f,h,j) shows samples exposed for 15 weeks. PP<sub>thermo</sub> [Fig. 6(a,b)], even after only 3 weeks of exposition, did not show any plastic deformation before fracture. After 15 weeks of exposition, PP<sub>thermo</sub> presented a very degraded layer next to the surface exposed directly to UV radiation; this indicated a more fragile fracture. These micrographs observations were in good agreement with the impact strength results [Fig. 2(d)]. The impact strength of HIPS presented similar values to the ones of PP samples exposed to UV radiation. However, the fracture surface was completely different, as shown in Figure 6(c,d). In this case, the fracture mechanism was governed by a large field of crack propagation, characteristic of a fragile matrix toughened by rubber particles.<sup>31</sup> After 15 weeks of exposition, the fracture surface of HIPS changed

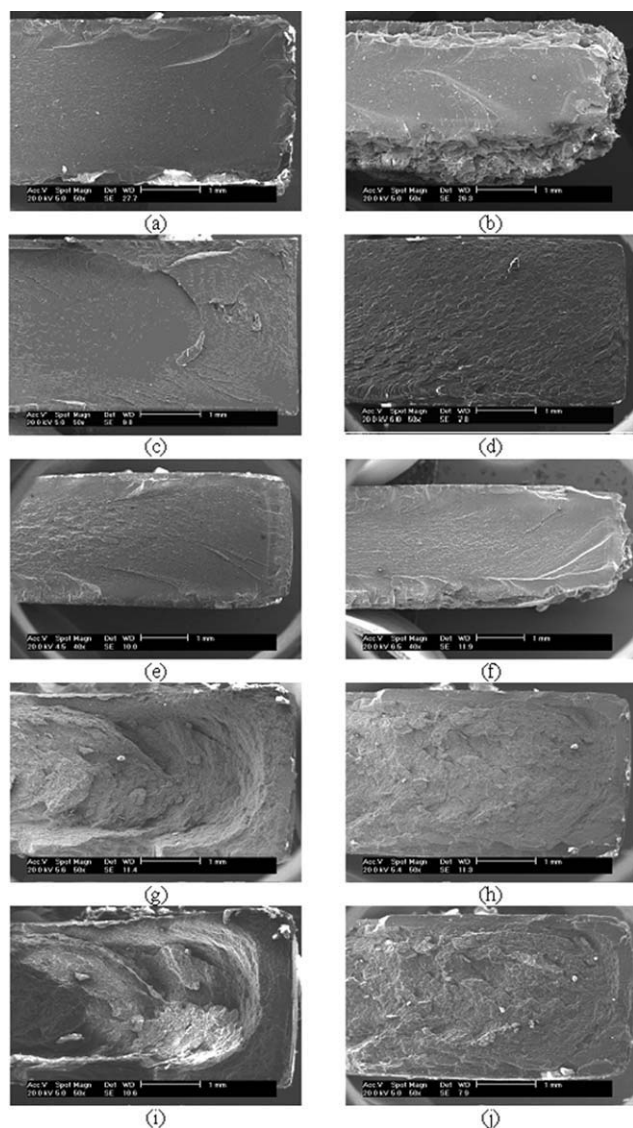


**Figure 6** Fracture surfaces from the crack-initiation zone of the neat PP<sub>thermo</sub> exposed for (a) 3 and (b) 15 weeks, neat HIPS exposed for (c) 3 and (d) 15 weeks, 90/10 blend exposed for (e) 3 and (f) 15 weeks, 80/20 blend exposed for (g) 3 and (h) 15 weeks, and 70/30 blend exposed for (i) 3 and (j) 15 weeks.

compared to the sample exposed for only 3 weeks; however, the value of impact strength did not change significantly. Probably, the crosslink reactions of the rubber phase altered the fracture mechanism but not the absorbed energy during the analysis. As expected, the 90/10 blend presented a similar fracture surface to the one of PP [Fig. 6(e,f)], whereas the 80/20 and 70/30 blends [Fig. 6(g–j)] presented different surface fractures than PP and HIPS. The surface fractures of the 70/30 blend presented a singular topography similar to a twister. This event could be better visualized on micrographs from the crack-propagation zone of these samples exposed to UV radiation for 3 and 15 weeks (see Fig. 7). The 80/20 blend presented a similar behavior. The

micrographs revealed a different mechanism of fracture and showed a layer-to-layer twister formation that could absorb a higher energy during impact tests, even after 15 weeks of exposure, as shown in Figure 2(d).

### Photodegradation of the blends with SBS

Figure 8(a–d) presents the mechanical properties of the blends to which SBS was added and that were exposed for different durations of UV radiation. The values of the modulus of elasticity and stress at break were similar for all of the different composition blends before UV exposure. The values of strain at break and impact strength were larger for lower dispersed phase concentration, but the difference between these values for the 90/10 and 70/30 blends were smaller than in the case of the noncompatibilized blends. These results indicate that SBS prevented coalescence of the dispersed phase.

Different from what was observed for the binary blends, it seems that the increase of time of exposure for times greater than 3 weeks did not significantly affect the values of modulus of elasticity and stress at the break point [see Fig. 8(a,b)] of the blends with SBS. As shown in Figure 8(c,d), with 3 weeks of exposure, the strain at break and impact strength underwent a great drop, but after that, the values were not greatly affected by the irradiation time. In particular, the strain at the break point [Fig. 8(c)] for all of the blends with SBS, even after 15 weeks, presented larger values for the binary blends; this indicated the efficiency of SBS as a compatibilizer. However, blends with SBS did not have better values of impact strength than the noncompatibilized one when the sample was exposed to UV radiation. Blends without SBS after 15 weeks of exposure presented a large and fragile degraded layer on the surface, whereas blends with SBS submitted to the same conditions presented a smaller and less fragile one (see the differences of morphology of the surface in Figs. 6 and 9). In the case of the blends without SBS, the degraded layer was so fragile that it prevented stress transfer during the impact test. In this case, the impact strength measured corresponded

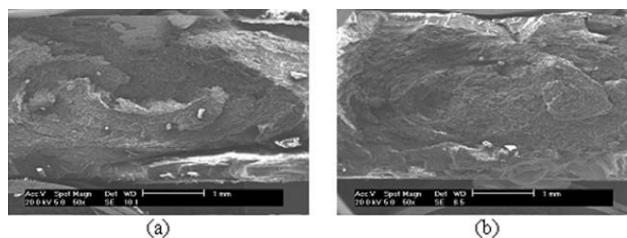


**Figure 7** Fracture surfaces from the crack-propagation zone of the 70/30 blend exposed for (a) 3 and (b) 15 weeks.



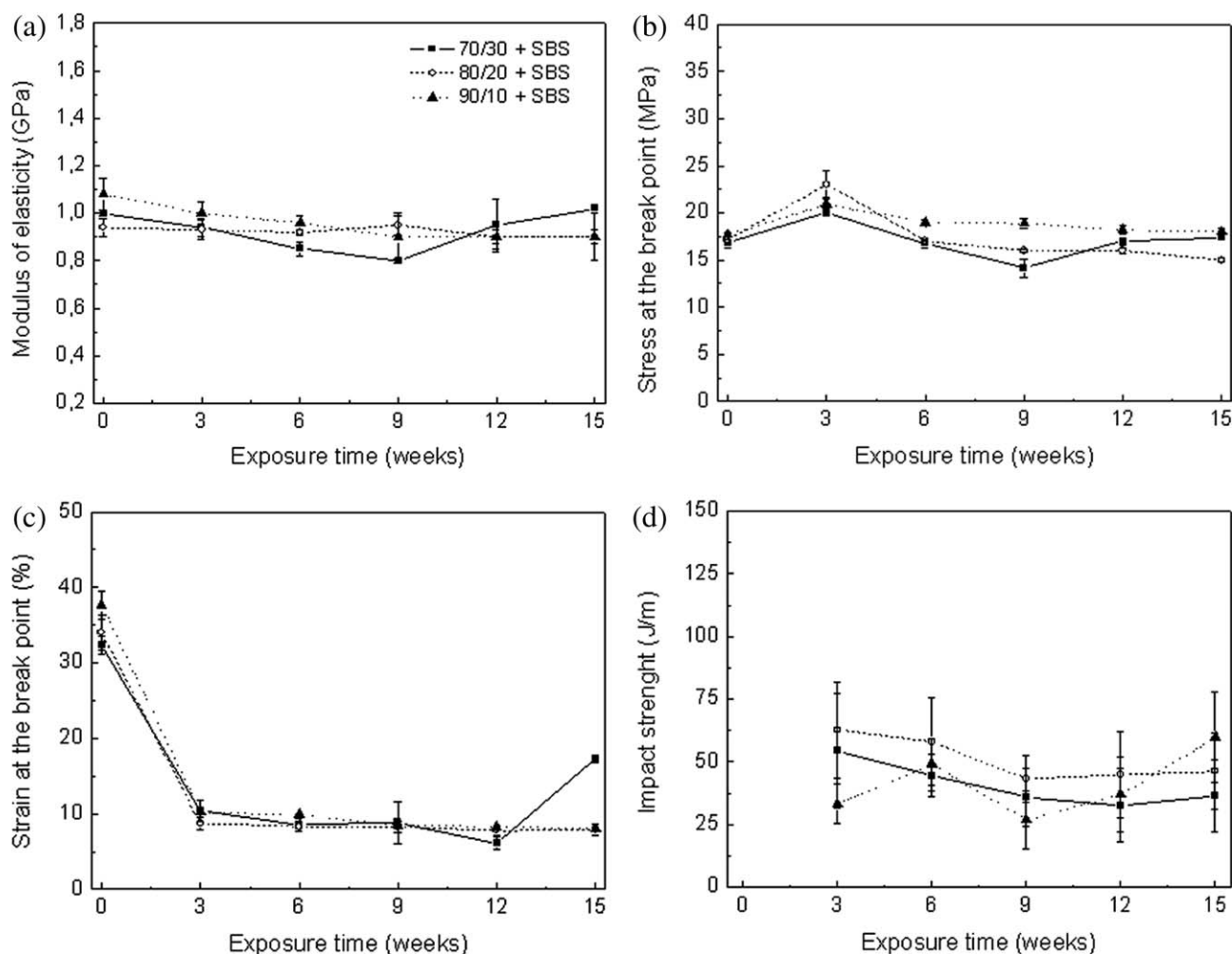


**Figure 8** Mechanical properties of the blends with the addition of SBS: (a) modulus of elasticity, (b) stress at the break point, (c) strain at the break point, and (d) impact strength as functions of the time of UV exposure.

only to the nondegraded material (bulk). In the case of the blends containing SBS, the impact strength measured corresponded to both the degraded layer and the bulk of the material; this resulted in a smaller value than in the former case. Similar results have been observed for PP,<sup>8</sup> polystyrene,<sup>29</sup> and PS/montmorillonite nanocomposites.<sup>32</sup>

Figure 9 shows micrographs of the fractures of the impact samples (crack-initiation zone) of the blends to which SBS was added and that were exposed to UV radiation for 3 and 15 weeks. Figure 9(a,c,e) presents samples exposed for 3 weeks, and Figure 9(b,d,f) presents samples exposed for 15 weeks. When Figure 9(a,c,e) is compared Figure 6(a,c,e), it is clear that the fracture surfaces of all of the blends to which SBS was added were completely different from the ones without SBS. The twister observed for the 70/30 blend was not observed when SBS was added to the blends (see the crack-propagation zones in Fig. 10). This layer-to-layer twister formation, observed in Figure 6, could have been obtained

during the filling of the injection mold because of the lack of adhesion between PP and HIPS. As also shown in Figure 9, the morphology of the fractures of the samples that were exposed to UV light for 15 weeks were very similar to the ones of the fractures of the samples that were exposed for 3 weeks. These observations were in good agreement with the fact that the impact strength of the blends was not altered by UV exposure.

Figure 11 shows the values of MFI of the blends to which SBS was added and that were exposed to UV radiation for different times. The values of MFI for the blends to which SBS was added were lower than the ones for the blends without SBS; this indicated the role of SBS as a compatibilizer or a smaller extent of photodegradation compared with blends without SBS.

Waldman and De Paoli<sup>20</sup> showed that the presence of a compatibilizer at high concentration (3 wt % with respect to the whole blend) increased the interfacial area between the phases and accelerated



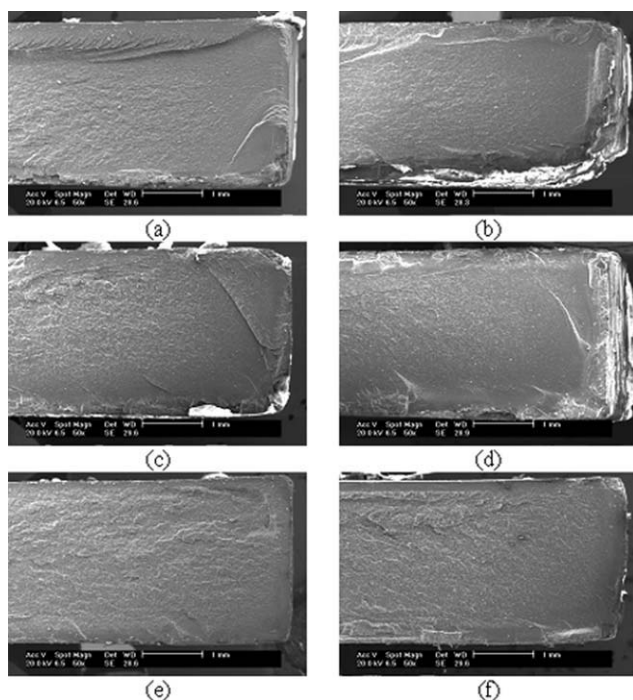


**Figure 9** Fracture surfaces from the crack-initiation zone of the blends with the addition of SBS: the 90/10 blend exposed for (a) 3 and (b) 15 weeks, 80/20 blend exposed for (c) 3 and (d) 15 weeks, and 70/30 blend exposed for (e) 3 and (f) 15 weeks.

the photodegradation process of PP/PS blends, whereas a low concentration (1 wt % with respect to the whole blend) reduced the occurrence of the phenomenon of energy transfer between the domains and slowed down the photodegradation process. The data from the blends with SBS showed better performance when compared with blends without SBS. Probably, the concentration of SBS used was low, and this resulted in a photostabilization of the

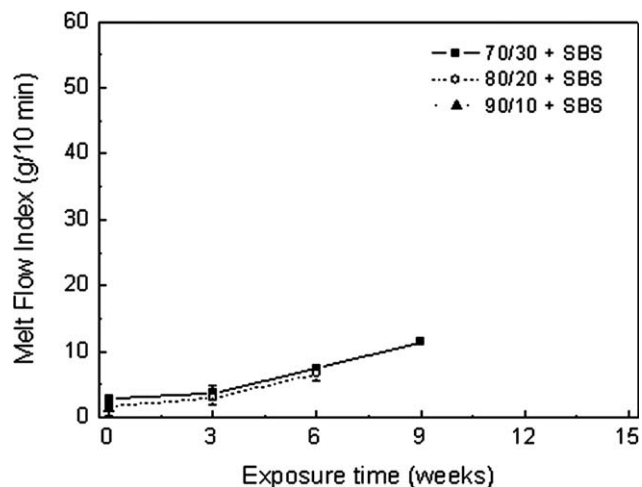


**Figure 11** MFIs for the blends with the addition of SBS as a function of the time of UV exposure.

blend from the reduction of energy transfer between the domains of PP and HIPS.

## CONCLUSIONS

In this study, the photodegradation of several PP/HIPS blends (with concentrations ranging from 90/10 to 70/30) with and without the addition of SBS was examined. The evolution of the mechanical properties, surface fractures, and melt flow indices of the blends as a function of time of exposure was evaluated.

The modulus of elasticity, tensile strength, strain, and impact strength decreased upon UV exposure for all of pure materials and blends. This decrease was much larger for the individual components during the first 3 weeks of exposure, as the individual components presented much larger values of mechanical strengths than the blends before degradation. However, after 3 weeks of UV exposure, all of

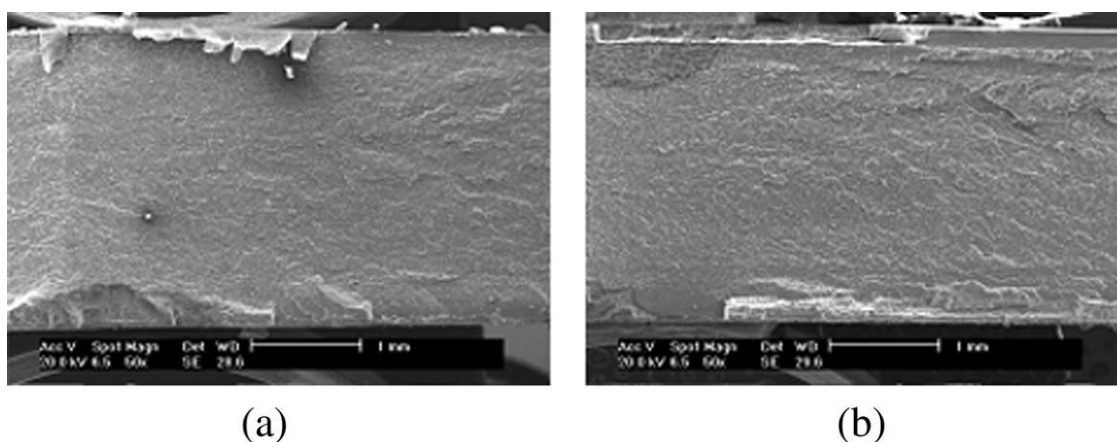


**Figure 10** Fracture surfaces from the crack-propagation zone of the 70/30 blend exposed for (a) 3 and (b) 15 weeks with the addition of SBS.

the materials presented values of mechanical properties within the same order of magnitude. After 3 weeks of UV exposure, an increasing concentration of HIPS resulted in a smaller decrease in the mechanical properties. This decrease was even smaller for the blends to which SBS was added. The better photostability of the blends was most likely due to the opacity of the materials and to the larger scattering effect of the interface between the polymers forming the blends. The smaller decreases in the impact strengths of the larger HIPS concentration blends originated from a different morphology.

FTIR analyses showed that UV exposure of the blends resulted in the occurrence of carbonyl bounds within the components of the blends.

The evaluation of MFI of the materials exposed to UV light indicated that more carbonyl and hydroperoxyl groups were formed for the 90/10 and 80/20 blends. The addition of SBS resulted in a smaller decrease of MFI upon UV exposure; this was most likely due either to the compatibilizing effect of SBS for PP/HIPS blend or to a smaller decrease in the molar mass of the blends.

Some of the observations made in this study were justified by energy transfer between the blend domains during UV exposure. The energy transfer between blend domains could be explained as a faster photodegradation of the blends compared to those of the individual components. However, this effect seemed to be minimized, depending on the thickness of the samples.

## References

1. Huang, S. J. *J Macromol Sci Pure Appl Chem* 1995, 32, 593.
2. Burillo, G.; Clough, R. L.; Czvikovszky, T.; Guven, O.; Le Moel, A.; Liu, W.; Singh, A.; Yang, J.; Zaharescu, T. *Radiat Phys Chem* 2002, 64, 41.
3. La Mantia, F. P. *Polym Degrad Stab* 1993, 42, 213.
4. Gross, R. A.; Kalra, B. *Science* 2002, 297, 803.
5. Cornell, D. D. *J Polym Environ* 2007, 15, 295.
6. Santana, R. M. C.; Manrich, S. *J Appl Polym Sci* 2003, 88, 2861.
7. Horak, Z.; Fort, V.; Hiavatá, D.; Lednický, F. *Polymer* 1996, 37, 65.
8. Rabello, M. S.; White, J. R. *Polym Degrad Stab* 1997, 56, 55.
9. Rabello, M. S.; White, J. R. *Polymer* 1997, 38, 6379.
10. Fechine, G. J. M.; Demarquette, N. R. *Polym Eng Sci* 2008, 48, 365.
11. Ghaffar, A.; Scott, A.; Scott, G. *Eur Polym J* 1976, 12, 615.
12. Ghaffar, A.; Scott, A.; Scott, G. *Eur Polym J* 1977, 13, 83.
13. Ghaffar, A.; Scott, A.; Scott, G. *Eur Polym J* 1977, 13, 89.
14. Ghaffar, A.; Scott, A.; Scott, G. *Eur Polym J* 1975, 11, 271.
15. Torikai, A.; Sekigawa, Y.; Fueki, K. *Polym Degrad Stab* 1988, 21, 43.
16. Kaczmarek, H.; Kowalonek, J.; Klusek, Z.; Pirzgalski, S.; Datta, S. *J Polym Sci Part B: Polym Phys* 2004, 42, 585.
17. Kaczmarek, H.; Podgórski, A.; Bajer, K. *J Photochem Photobiol A* 2004, 171, 187.
18. Kaczmarek, H. *Polymer* 1996, 37, 547.
19. Saron, C.; Sanchez, E. M. S.; Felisberti, M. I. *J Appl Polym Sci* 2007, 104, 3269.
20. Waldman, W. R.; De Paoli, M. A. *Polym Degrad Stab* 2008, 93, 273.
21. Demarquette, N. R.; Souza, A. M.; Palmer, G.; Macaúbas, P. H. P. *Polym Eng Sci* 2003, 43, 670.
22. Demarquette, N. R. *Int Mater Rev* 2003, 48, 247.
23. Wu, S. *Polym Eng Sci* 1990, 30, 753.
24. Valera, T. S.; Demarquette, N. R. *Eur Polym J* 2008, 44, 755.
25. Macaubas, P. H. P.; Demarquette, N. R. *Polymer* 2001, 42, 2543.
26. Perkins, W. G. *Polym Eng Sci* 1999, 39, 2445.
27. Carlsson, D. J.; Wiles, D. M. *J Macromol Sci Rev Macromol Chem* 1976, 14, 65.
28. Rabek, J. F. *Polymer Photodegradation*; Chapman & Hall: London, 1995.
29. Souza, A. R.; Amorin, K. L. E.; Medeiros, E. S.; Mélo, T. J. A.; Rabello, M. S. *Polym Degrad Stab* 2006, 91, 1504.
30. Allen, N. S.; Edge, M. *Fundamentals of Polymer Degradation and Stabilization*; Elsevier Science: New York, 1992.
31. Wu, S. *J Polym Sci* 1983, 21, 699.
32. Oliveira, C. F. P.; Carastan, D. J.; Demarquette, N. R.; Fechine, G. J. M. *Polym Eng Sci* 2008, 48, 1511.